

Identification of Mechanisms of Resistance to ALK Inhibitors. Next-generation sequencing-based liquid biopsy profiling: A step towards personalized treatment.

Estela Sánchez-Herrero

Hospital Universitario Puerta del Hierro Majadahonda

Roberto Serna-Blasco

Hospital Universitario Puerta de Hierro Majadahonda

Vadym Ivanchuk

Hospital Universitario Puerta de Hierro Majadahonda

Rosario García-Campelo

Complejo Hospitalario Universitario de La Coruña: Complejo Hospitalario Universitario A Coruna

Manuel Dómine

Fundación Jiménez Díaz: Hospital Universitario Fundación Jimenez Diaz

José Miguel Sánchez

Hospital Universitario de la Princesa

Bartomeu Massuti

Alicante General University Hospital: Hospital General Universitari d'Alacant

Noemi Reguart

Clinic Barcelona Hospital University: Hospital Clinic de Barcelona

Carlos Camps

General University Hospital Consortium of Valencia: Consorci Hospital General Universitari de Valencia

Sandra Sanz-Moreno

Hospital Universitario Puerta de Hierro Majadahonda

Silvia Calabuig-Fariñas

Consorci Hospital General Universitari de València: Consorci Hospital General Universitari de Valencia

Eloísa Jantus-Lewintre

Consorci Hospital General Universitari de València: Consorci Hospital General Universitari de Valencia

Magdalena Arnal

Hospital del Mar Institute for Medical Research: Institut Hospital del Mar d'Investigacions Mediques

Dietmar Fernández-Orth

Center for Genomic Regulation: Centre de Regulacio Genomica

Víctor González-Rumayor

Atrys Health

Virginia Calvo

Hospital Universitario Puerta de Hierro Majadahonda

Mariano Provencio

Hospital Universitario Puerta de Hierro Majadahonda

Atocha Romero (✉ atocha10@hotmail.com)

Hospital Universitario Puerta del Hierro Majadahonda

Research

Keywords: Alectinib, ALK, ALK-TKI, Brigatinib, Ceritinib, Crizotinib, EML4-ALK, Liquid Biopsy, NGS, NSCLC

Posted Date: October 8th, 2020

DOI: <https://doi.org/10.21203/rs.3.rs-86055/v1>

License: © ⓘ This work is licensed under a Creative Commons Attribution 4.0 International License. [Read Full License](#)

Abstract

Background: Despite impressive and durable responses, patients treated with ALK inhibitors (ALK-Is) ultimately progress. We investigated potential resistance mechanisms in a series of ALK-positive non-small cell lung cancer (NSCLC) patients progressing on different types of ALK-Is.

Methods: 26 plasma and 2 cerebrospinal fluid samples collected upon disease progression to an ALK-I, from 24 advanced ALK-positive NSCLC patients, were analyzed by next-generation sequencing (NGS). A tool to retrieve variants at the ALK locus was developed.

Results: 61 somatic mutations were detected in 14 genes: TP53, ALK, PIK3CA, SMAD4, MAP2K1 (MEK1) FGFR2, FGFR3, BRAF, EGFR, IDH2, MYC, MET, CCND3 and CCND1. Overall, We identified at least one mutation in ALK locus in 10 (38.5%) plasma samples, being the G1269A and G1202R mutations the most prevalent among patients progressing to first- and second-generation ALK-I treatment, respectively. An exon 19 deletion in EGFR was identified in a patient showing primary resistance to ALK-I. Likewise, the G466V mutation in BRAF and the F129L mutation in MAP2K1 (MEK1) were identified as the underlying mechanism of resistance in three patients who gained no or little benefit from second-line treatment with an ALK-I. Putative ALK-I resistance mutations were also found in PIK3CA and IDH2. Finally, a c-MYC gain, along with a loss of CCND1 and a FGFR3, were detected in a patient progressing on a first-line treatment with crizotinib.

Conclusions: NGS analysis of liquid biopsies upon disease progression identified putative ALK-I resistance mutations in most cases, being a valuable approach to devise therapeutic strategies upon ALK-I failure.

Background

Anaplastic lymphoma kinase inhibitors (ALK-Is) have dramatically improved outcomes of non-small cell lung cancer (NSCLC) patients whose tumors harbor an ALK translocation (1, 2). A broad therapeutic arsenal is currently available to treat ALK-positive NSCLC tumors, and sequential treatment with different ALK-Is is the best therapeutic option for NSCLC patients with an ALK translocation (3, 4). However, it remains unclear how ALK-Is should be sequenced in order to maximize survival and quality of life. It has been proposed that treatment sequencing can be established according to clinical characteristics of the patients or toxicity profile. In this way, second generation ALK-Is have shown impressive central nervous system (CNS) efficacy in ALK-positive NSCLC patients (5, 6). On the other hand, crizotinib is associated with adverse events dominated by gastrointestinal and visual effects, increased transaminases and edema, whereas the most common adverse events of alectinib are anemia, myalgia and increased blood bilirubin (7). The tumor molecular profile can also determine the treatment response. In this way, among patients treated with the ALK-I lorlatinib, the ALK fusion variant 3 was associated with significantly longer progression-free survival than variant 1 (8). Finally, several resistance mutations have been identified upon progression to an ALK-I (9, 10). While some of them confer resistance to specific ALK-Is, others do not (11–13). Paradoxically, therapy is seldom decided based on the tumor molecular profile upon disease progression, and ALK-Is are usually prescribed empirically. Conversely, biomarker testing after treatment failure is routinely performed in EGFR-positive NSCLC patients, as recommended by clinical guidelines (14).

Repeat tumor biopsy upon disease progression is not always feasible. Nevertheless, there is considerable evidence showing that genotyping cell-free DNA (cfDNA) is a valid and significantly faster approach than genotyping solid biopsies. Next-generation sequencing (NGS) enables the interrogation of a large number of mutations and can be used with liquid biopsies (15). Moreover, NGS can also provide information about concomitant mutations that might be of prognostic significance.

In this study, we have analyzed 26 plasma and 2 cerebrospinal fluid (CSF) samples, from 24 patients, collected upon disease progression while being treated with an ALK-I, in order to determine the clinical utility of liquid biopsies for ALK-Is sequencing. In addition, we provide a pipeline specifically designed to detect somatic mutations in the ALK domain. Finally, we evaluate the clinical significance of somatic alterations in genes other than ALK.

Methods

Study population

Between June 2015 and July 2019, 24 stage IV, ALK-positive NSCLC patients progressing on an ALK-I (the ALK-cohort), were prospectively recruited from six hospitals across Spain. The study protocol was approved by the Hospital Puerta de Hierro Ethics Committee (internal code 79 – 18), and was conducted in accordance with the precepts of the Code of Ethics of The World Medical Association (Declaration of Helsinki). All patients provided their appropriate written informed consent to participate in the study prior to enrollment. Briefly, patients who were 18+ years of age and with a pathologically confirmed diagnosis of stage IV NSCLC with an EML4-ALK translocation were eligible for inclusion. All samples were collected upon disease progression, which was assessed according to RECIST criteria v.1.1. In total, 26 plasma and 2 CSF specimens were collected and analyzed.

Laboratory procedures

Peripheral whole-blood samples were collected in a 10-mL Streck Cell-Free DNA BCT® (Streck, USA) tube for cfDNA. CSF samples were collected in a 10-mL sterile tube with no additives or anticoagulants. Samples were centrifuged at room temperature in two consecutive centrifugations of 1500 *g* for 10 min and 5000 *g* for 20 min in order to separate plasma or CSF from the cellular fraction. cfDNA was isolated using QIAamp Circulating Nucleic Acid Kit (QIAGEN, Valencia, CA, USA) according to the manufacturer's instructions. All samples were stored immediately at – 80 °C until cfDNA genotyping.

Libraries were prepared from at least 10 ng of cfDNA using the OncoPrint™ Pan-Cancer Cell-Free Assay kit (Thermo Fisher, Palo Alto, CA, USA) according to the manufacturer's instructions. This amplicon-based targeted-sequencing assay allows the detection of multiple biomarkers in tumor-derived DNA and RNA isolated from liquid biopsy samples with a limit of detection (LOD) down to an allele frequency (AF) of 0.1%. Specifically, the panel includes 52 genes

frequently mutated in cancer, in which hotspots (single nucleotide variants; SNVs), fusions, copy-number variations (CNVs) and exon skipping can be studied. AMPureXP magnetic beads (Beckman Coulter, Inc., Brea, CA, USA) were used to purify all libraries. Subsequently, the individual libraries were quantified using the Ion Library TaqMan® Quantitation Kit (Thermo Fisher, Palo Alto, CA, USA) in a StepOnePlus™ qPCR machine (Thermo Fisher, Palo Alto, CA, USA) and adjusted to a final concentration of 50 pM. Eight samples were pooled. Templating and Ion 550™ Chip loading were carried out with an Ion Chef™ System (Thermo Fisher, Palo Alto, CA, USA). Finally, an Ion GeneStudio™ S5 Sequencer (Thermo Fisher, Palo Alto, CA, USA) was used to sequence loaded Ion 550™ chips.

The mutations identified by NGS were confirmed by digital PCR (dPCR) on cfDNA samples using a QuantStudio® 3D Digital PCR System (Applied Biosystems, South San Francisco, CA, USA). In accordance with the manufacturer's specifications, dPCR reactions were performed in an 18-µL volume comprising 9 µL of 20X QuantStudio 3D Master Mix, 0.45 µL of 40X commercially available predesigned or custom TaqMan® assays and 8.55 µL of cfDNA. Subsequently, 14.5 µL of the PCR reaction were loaded onto a QuantStudio 3D Digital PCR 20K chip using QuantStudio™ 3D Digital PCR Chip Loader. Each dPCR run included a negative control DNA, as a wild-type (wt) control, a blank (with no cfDNA) and a positive control. PCR reactions were performed in a thermal cycler (Applied Biosystems) at 96 °C for 10 min, then 40 cycles at 56 °C for 2 min and 98 °C for 30 s, and a final elongation step at 72 °C for 10 min. Finally, samples were maintained at 22 °C for at least 30 min. After dPCR was completed, chips were read using two independent QuantStudio™ 3D Digital PCR Instruments and the fluorescence was read twice. Results were visualized and analyzed using QuantStudio® 3D Analysis Suite™ Cloud Software and the automatic call assignments for each data cluster were manually adjusted when needed. The mutant allele frequency (MAF) was calculated as the ratio of mutant DNA molecules to the sum of mutant and wild-type (wt) DNA molecules.

Torrent Suite Software (v5.12) was used to analyze the raw sequencing data. The CoverageAnalysis (v. 5.12.0.0) plugin was used for sequencing coverage analysis (Thermo Fisher, Palo Alto, CA, USA). As recommended by the manufacturer, a median read coverage > 25,000 and a median molecular coverage > 2500 were required to detect a variant with a MAF of 0.1%. Raw reads were aligned to the human reference genome hg19. Variant calling, annotation and filtering were performed on the Ion Reporter (v5.10) platform using the OncoPrintTagSeq Pan-Cancer Liquid Biopsy workflow (v2.1). Briefly, sequencing reads were mapped to defined target regions (OncoPrint Pan-Cancer DNA Regions v1.0 (5.10)) and subjected to variant calling using OncoPrint Pan-Cancer Annotations v1 r. 0. All candidate mutations were manually reviewed using the Integrative Genomics Viewer v.2.3.40 (IGV), (Broad Institute, Cambridge, MA, USA). The clinical significance of somatic variants was determined according to the Standards and Guidelines for the Interpretation and Reporting of Sequence Variants in Cancer (16).

To detect variants in the *ALK* locus, we analyzed data by developing a bioinformatic pipeline, called the **VALK tool**, which is capable of fully automating the filtering of mutations in the *ALK* locus and generating a .csv file containing the output variants and a list of their properties. To increase the detection rate for variants at the *ALK* locus, specific conditions for SNVs, indels, multiple-nucleotide polymorphisms (MNP), fusions and copy-number variation (CNV) calls were defined. The pipeline uses the raw data in the non-filtered-oncoPrint.tsv, which contains variants that have passed the OncoPrint Variants (v.5.12) filter and variants that have not. Briefly, parameters such as the LOD, mutant allele frequency, molecular coverage of the mutant allele, number of reads supporting a specific variant, and clinical significance, among others, were considered in the selection of the different thresholds. Detailed information about the pipeline is available in the **Supplementary Methods** and in **Supplementary Fig. 1**. Positive and negative percentage agreement (PPA and NPA) and overall rates of agreement (ORA) of the **VALK tool** for detecting the *ALK* mutations specified in **Supplementary Table 1** were calculated considering the imperfect reference standard the dPCR result, using the two independent data sets, the *ALK* cohort and the Valencia cohort, which consists of 53 cfDNA samples from NSCLC patients.

Statistical analysis

Median follow-up was estimated by the reverse Kaplan–Meier method. Overall survival (OS) was defined as the time from the start of treatment with an *ALK* inhibitor to death or last follow-up. Progression-free survival (PFS) was defined as the time between the start of an *ALK*-inhibitor and disease progression (as ascertained by RECIST criteria), death, or the censored date of the last assessment, whichever occurred first. The log-rank test was used to assess statistical differences between Kaplan–Meier survival curves. Hazard ratios (HRs) were estimated from the Cox model using a multivariable approach adjusted for sex, Cooperative Oncology Group (ECOG) performance status, and lines of *ALK*-TKI. Association between clinicopathological variables and genomic features were assessed by Fisher's exact test. Values of $P < 0.05$ were considered statistically significant. Statistical analyses were performed using Stata 15.1.

Results

Study cohort.

We collected and analyzed 26 plasma and 2 cerebrospinal fluid (CSF) specimens from 24 metastatic patients diagnosed with an *ALK*-positive NSCLC who were progressing on an *ALK*-I. Baseline clinicopathological characteristics of the study population ($N = 24$) are presented in Table 1. The median age at diagnosis was 53 years (range, 36–72 years) and 58.3% were females. The majority of the patients were never-smokers (62.5%) and the most frequent histology was adenocarcinoma (95.8%). ECOG Performance Status at study entry varied from 0 to 2. As shown in Fig. 1, two samples from two patients were collected upon disease progression while on two consecutive lines of treatment with an *ALK*-I; three samples were obtained from one patient upon failure to three consecutive lines of *ALK*-I; all 21 other members of the cohort each provided a single sample.

Table 1
Baseline characteristics of the study cohort.

Feature		N	%
Age of Diagnosis (years)	Median (range)	53(36–72)	
Sex	Male	10	41.7%
	Female	14	58.3%
Smoking Status	Current smoker	3	12.5%
	Ex-smoker	6	25%
	Never-smoker	15	62.5%
ECOG Performance Status	0	12	50%
	1	11	45.8%
	2	1	4.2%
Histology	Adenocarcinoma	23	95.8%
	Neuroendocrine carcinoma	1	4.2%
Clinical Stage at diagnosis	III	6	25%
	IV	18	75%

As presented in Fig. 1, 13 samples corresponded to ALK-I-naïve patients who progressed on a first-line crizotinib (N = 11) or alectinib (N = 2) treatment. For these patients, the median PFS and OS were 11.6 months (95%CI: 6.5–20.9 months) and 24.6 months (95%CI: 11.8-NR months), respectively. In addition, 12 samples corresponded to patients who had received previously crizotinib and were treated with a second-generation ALK-I. Finally, the cohort included two samples from patients progressing on lorlatinib after failure of a prior second generation ALK-I and one patient progressing on alectinib who had previously received crizotinib plus two second generation ALK-I. Detailed information about treatment lines is presented in **Supplementary table 2**. The median PFS and OS for patients progressing on a second or subsequent line with an ALK-I were 5.4 months (95%CI: 2-9.1) and 11.2 months (95%CI: 3-NR) months respectively.

Next-generation sequencing analysis upon disease progression.

Overall, using the Pan-Cancer Cell-Free Assay, 61 somatic variants in ctDNA from 24 samples were detected. There were no significant differences in cfDNA input between samples in which a somatic mutation was detected in the cfDNA and those in which it was not (N = 4). One of the patients with undetectable plasma ctDNA had progressed exclusively at the brain level. The average number of mutations per patient was 2.18 and the median MAF was 0.39%. As expected, SNPs were the most frequent mutation type (N = 48). In addition, we identified 10 indels and three CNVs (Fig. 2). Specifically, a c-MYC gain in conjunction with a CCND1 and an FGFR3 loss were detected in a patient progressing on a first line with crizotinib. This patient also harbored a mutation in TP53 (Fig. 2).

As illustrated in Fig. 2, somatic mutations were detected in 14 genes: TP53, ALK, PIK3CA, SMAD4, MAP2K1 (MEK) FGFR2, FGFR3, BRAF, EGFR, IDH2, MYC, MET, CCND3 and CCND1. All the variants detected are listed in **Supplementary Table 3**. Thirteen variants (12 of which were in the ALK locus and one was in the EGFR gene) were categorized as being of strong clinical significance.

Identification of acquired resistance mutations in the ALK locus upon disease progression

To increase the sensitivity for detecting somatic mutations in the ALK locus from ctDNA we developed an algorithm (**VALK tool**) for this purpose (available upon request). The tool has been specifically designed for the analysis of the NGS data obtained from liquid biopsies. Among other parameters, the algorithm takes into account the molecular depth and molecular counts as well as specific regions that are more likely for false positive calls. In order to test the analytical performance of the tool, all SNPs in the ALK locus that were present in the non-filtered-oncomine.tsv file were analyzed by dPCR. In total, 19 ALK variants from 22 samples were analyzed by dPCR (**Supplemental Table 1**). Considering the non-reference standard the dPCR result PPA, NPA, and overall percent agreement of ALK mutation detection for the **VALK tool** were 67% (95%CI: 35–90%), 93% (95%CI: 75–99%), and 85% (95%CI: 69–94%), respectively. The algorithm was tested further in a second independent batch of 53 samples provided by a different laboratory (Valencia cohort). In this case the PPA, NPA, and overall percent agreement were 100% (95%CI: 16–100%), 98% (95%CI: 90–100%), and 98% (95%CI: 90–100%), respectively.

Overall, in the ALK-cohort we detected at least one ALK mutation in 10 (38.5%) plasma samples collected upon disease progression (Table 2, **Supplementary Fig. 2**). Notably, the Oncomine variants v5.10 filter only detected ALK mutations in three patients (Table 2).

Table 2
Somatic mutations detected at the ALK locus upon treatment failure.

Nº of patient	Nucleotide Change	Amino Acid Change	Progression to	Line of treatment	Filter	MAF dPCR (%)
Patient 2	c.3599C > T	p.A1200V	Crizotinib	First line	non-filtered-oncomine.tsv	0.038
Patient 3	c.3806G > C	p.G1269A	Crizotinib	First line	Oncomine 5.10/VALK tool	2.816
Patient 5	c.3806G > C	p.G1269A	Crizotinib	First line	Oncomine 5.10/VALK tool	0.422
Patient 5	c.3604G > A	p.G1202R	Ceritinib	Second line	Oncomine 5.10/VALK tool	2.117
Patient 6	c.3586C > A	p.L1196M	Crizotinib	First line	non-filtered-oncomine.tsv	0.056
Patient 16	c.3617C > A	p.S1206Y	Alectinib	Second line	VALK tool	0.005
Patient 16	c.3604G > A	p.G1202R	Alectinib	Second line	VALK tool	0.038
Patient 19	c.3586C > A	p.L1196M	Lorlatinib	Third line	non-filtered-oncomine.tsv	0.049
Patient 19	c.3824G > A	p.R1275Q	Lorlatinib	Third line	non-filtered-oncomine.tsv	0.044
Patient 20	c.3604G > A	p.G1202R	Alectinib	Second line	VALK tool	0.324
Patient 22	c.3604G > A	p.G1202R	Alectinib	Fourth line	VALK tool	0.011
Patient 24	c.3538G > C	p.V1180L	Alectinib	First line	non-filtered-oncomine.tsv	0.350

The G1202R mutation was the most prevalent among patients treated with a second-generation ALK-I (N = 15), being identified in four patients who had progressed on alectinib (N = 3) and ceritinib (N = 1). The S1206Y mutation was detected along with the G1202R mutation in one of the aforementioned alectinib-progressing patients. This patient had been treated with crizotinib before initiating alectinib treatment. The low MAF of the S1206Y mutation suggests that it could be responsible for the previous crizotinib failure. In addition, the G1269A mutation was detected upon crizotinib failure in two cases and the L1196M mutation was identified after progression to crizotinib and lorlatinib. The latter was detected together with the R1275Q mutation in a patient diagnosed with an ALK-positive neuroendocrine carcinoma. Finally, the A1200V mutation (N = 1) arose as a result of the failure of crizotinib, and the V1180L mutation (N = 1) was detected in a patient progressing on a first-line treatment with alectinib (Table 2).

Other molecular mechanisms underlying resistance to ALK-I.

A deletion in exon 19 of the EGFR gene, a non-V600 BRAF mutation and the F129L mutation in MAP2K1 (MEK1) were identified in four patients who showed no objective survival benefit from ALK-Is. None of these patients had a secondary mutation in ALK locus.

Notably, the patient harboring the E746_A750del mutation in the EGFR gene had a PFS time of 1.8 months under first-line crizotinib treatment. The patient was subsequently treated with alectinib but tumor progression was assessed 3.1 months later prompting a switch of treatment to lorlatinib, but that also failed after 1.8 months, suggesting that the tumor had primary resistance to ALK-Is (Fig. 1, Table 3). Similarly, a non-V600 BRAF mutation, namely G466V, was identified in the CFS collected upon disease progression to ceritinib. Remarkably, while PFS with first-line crizotinib was 21 months, disease progression was assessed within 3 months of starting second-line ceritinib treatment (Fig. 1), suggesting that the G466V mutation was acquired promoting resistance to second-line ALK-Is. Likewise, two patients harboring the F129L mutation in MAP2K1 (MEK1) obtained little benefit from second-line ALK-I (Fig. 1, Table 3). This mutation was detected upon disease progression to alectinib and lorlatinib. Noteworthy, the median PFS and OS for second-line treatment for these patients were less than one month (0.97) and 3 months, respectively, whereas median the PFS and OS for patients progressing on a second or subsequent lines with an ALK-I but without mutations in MAP2K1 were 5.9 and 11.2 months (P log rank < 0.05 in both cases; **supplementary Fig. 3**).

Table 3
Resistance mutations detected in loci other than ALK upon tumor progression.

Patient	Treatment	Treatment Line	Sample	HUGO Symbol	Amino Acid Change	Nucleotide Change / CNV	Type	Variant Class (Tier)	Transcript
Patient 8	Alectinib	1st	Sample 10	IDH2	p.R140Q	c.419G > A	SNV	Potential Clinical Significance	NM_00216
Patient 14	Ceritinib	2nd	Sample 16	PIK3CA	p.E545K	c.1633G > A	SNV	Potential Clinical Significance	NM_00621
Patient 18	Brigatinib	2nd	Sample 20	PIK3CA	p.E545A	c.1634A > C	SNV	Potential Clinical Significance	NM_00621
Patient 3	Ceritinib	2nd	Sample 4	BRAF	p.G466V	c.1397G > T	SNV	Potential Clinical Significance	NM_00433
Patient 10	Alectinib	2nd	Sample 12	MAP2K1	p.F129L	c.385T > C	SNV	Potential Clinical Significance	NM_00275
Patient 12	Crizotinib	1st	Sample 14	MYC		Gain (3,08)	CNV	Potential Clinical Significance	NM_00535
Patient 19	Crizotinib	1st	Sample 21	EGFR	p.E746_A750del	c.2235_2249delGGAATTAAGAGAAGC	InDel	Strong Clinical Significance	NM_00522
Patient 23	Lorlatinib	2nd	Sample 27	MAP2K1	p.F129L	c.385T > C	SNV	Potential Clinical Significance	NM_00275

Putative ALK-I resistance mutations were also found in IDH2, PIK3CA and MYC (Table 3). Specifically, the oncogenic mutations E545K and E545A in the PIK3CA gene were detected in the plasma sample of two patients progressing on ceritinib and brigatinib (Table 3). Likewise, the gain-of-function mutation in IDH2, R140Q, was detected upon disease progression to first-line alectinib treatment. Finally, as previously mentioned, a c-MYC amplification was detected jointly with a loss of CCND1 and of FGFR3.

Other concomitant mutations

In the present cohort, TP53 was the most frequently mutated gene. The frequency of TP53 mutations identified is presented in **Supplementary Fig. 4**. As shown, the P92A mutation accounted for 36.36% of mutations in this gene. Curiously, the median PFS was 7.7 months, for patients with tumors harboring the P92A mutation and progressing on a first-line ALK-I, compared with 14.7 months for patients in whom this mutation was not detected. Similarly, the median OS was 11.8 months for patients progressing on a first-line treatment with an ALK-I with tumors harboring the P92A mutation compared with 34.9 months for patients testing negative for this mutation. However, these differences were not statistically significant.

Discussion

ALK-Is have dramatically improved outcomes in NSCLC patients as well as in several other hematological and solid malignancies (17). However, despite the impressive responses they elicit, patients invariably relapse due to acquired resistance mutations. Solid biopsies remain the gold standard for biomarker testing. However, logistics for obtaining repeat tumor biopsies are complicated and seldom feasible since many patients are unable to endure an invasive procedure, which at the end of the day leads to an empirical prescription of sequential ALK-Is. Nevertheless, blinding sequential strategies might have a deleterious effect on patient's survival due to the incompletely overlapping ALK mutation coverage of different ALK-Is. In this exploratory analysis, we show, as proof of concept, that plasma NGS is feasible, enabling the detection of resistance mechanisms in patients with ALK-positive NSCLC upon progressive disease. We also provide an algorithm capable of retrieving somatic mutations in the ALK locus that would otherwise be discarded by the commercial bioinformatic pipeline. Remarkably, the developed algorithm performs well in terms of discarding samples with no mutations. Measuring the abundance of DNA molecules in a given sample by NGS is subjected to PCR amplification bias, as not all targeted amplicons are amplified with the same efficacy during library preparation. This limitation can be, at least partly, alleviated by ensuring that all molecules are distinguishable before amplification using unique molecular identifiers (UMIs)(18, 19). With this approach, instead of counting reads, reads are grouped by UMIs, where each distinct UMI identifies the original molecule. In this scenario, parameters such as molecular coverage and molecular counts are pivotal, however free bioinformatic tools, based on the optimization of these parameters remains lacking. As presented in Table 2, the commercial pipeline only detected 3 out of 12 mutations. MAFs of variants detected by the commercial pipeline were 2.8%, 2.1% and 0.4%. According to the manufacturer's specifications, the limit of detection, in terms of MAF, for mutations is 0.1%. However, in our hands, mutations with a MAF below 0.5% are seldom detected by the commercial pipeline. By using the VALK pipeline, some mutations that would otherwise have been missed can be rescued. Yet, confirmation using an alternative technique such as dPCR would be required to rule out false-positive calls.

Regarding acquired mutations in the ALK locus, our results are consistent with those of previous studies. Specifically, secondary mutations were detected in the plasma samples of 4 of the 11 (36%) patients treated with first-line crizotinib, with the G1269A mutation being detected in two cases. In this regard, mutation detection rate after crizotinib failure might vary from 60% (20) to 24% (21), G1269A being the most prevalent mutation. In this subset of patients we

also detected the L1196M and S1206Y mutations, which have been reported to occur in 7% and 2% of cases, respectively, of ALK-positive NSCLC patients treated with crizotinib (11). Finally, we detected the A1200V mutation after crizotinib failure in one patient. This mutation is also known to appear upon crizotinib progression (20). On the other hand, we found that the G1202R mutation was identified in 3 of the 10 patients (30%) progressing on alectinib. This mutation is known to arise mainly after treatment with second-generation ALK-Is (11). Recently, Johannes N et al reported a 53% ALK mutation detection rate in samples obtained post-progression on alectinib (22) in which G1202R was the most frequent mutation. In our cohort, more than one mutation in ALK locus was detected in two samples collected during second- and third-generation ALK-I treatment. Likewise, it has been described that ALK resistance mutations become more frequent with each successive generation of ALK-I as sequential treatment may promote the appearance of resistance mutation at the ALK locus (23).

A reduced number of studies analyzing samples collected upon progression to an ALK-I by NGS have so far been conducted (11, 19, 20), and the molecular mechanisms underlying treatment failure remains poorly understood. To our knowledge, we are the first group to evaluate the feasibility and clinical utility of the OncoPrint™ Pan-Cancer Cell-Free Assay, which is a relatively inexpensive panel. This panel detected somatic mutations in 14 genes: TP53, ALK, BRAF, PIK3CA, MAP2K1, FGFR2, FGFR3, EGFR, MYC, MET, IDH2, CCND3, CCND1 and SMAD4. Similarly, mutations in TP53, FGFR2, PIK3CA, MET have been identified in the tumor biopsy of patients progressing on ceritinib (11). The E545K and E545A mutations, which are two of the most common oncogenic mutations in PIK3CA, have also been detected upon progression in advanced EGFR-positive NSCLC patients (24). On the other hand, the IDH2 R140Q detected in our cohort is known to transform cells in vitro and induces myeloid and lymphoid neoplasms in mice (25, 26). The R149Q mutation in IDH2 is frequent in angioimmunoblastic T-cell lymphoma (27). In NSCLC, IDH1/2 mutations are rarely detected in primary tumors but it has been suggested that they could be branching drivers leading to subclonal evolution, based on the MAFs at which these mutations are detected (28). It is therefore not surprising that we found them upon treatment failure.

In addition, we found the E746_A750del mutation in one patient who did not benefit from treatment with ALK-Is. In this way, some researchers have found that mutations in EGFR in some NSCLC tumors coexist alongside ALK rearrangements (29) which may lead to primary resistance to ALK-I (30). Likewise, a non-V600 BRAF mutation was detected after 3 months of treatment with second-line ceritinib treatment, suggesting that resistance of the tumor to the ALK-I could be due to the acquisition of the BRAF mutation. It has been reported that ceritinib enhances the efficacy of trametinib, a MEK inhibitor, in BRAF/NRAS-wild type melanoma cell lines (31), which makes it plausible that ceritinib wouldn't have any effect in BRAF-mutated cells. Finally, two patients in whose plasma sample the F129L-activating mutation in MAP2K1 (MEK1) was detected, exhibited marked resistance to second- and third-generation ALK-Is. This mutation has been identified as the molecular mechanism underlying MEK/ERK pathway activation in resistant clones of human HT-29 colon cancer cells (32). Moreover, the activation of this downstream pathway is critical to the survival of ALK-positive NSCLC cells (33, 34). Indeed, the combination of ALK and MEK inhibition was highly effective at suppressing tumor growth in a preclinical model of EML4-ALK NSCLC (35). Taken together, it is plausible that the F129L-activating mutation in MAP2K1 is an acquired mutation that leads to tumor resistance to ALK-Is.

Mutations in the FGFR2 and FGFR3 genes were detected in two patients progressing on ALK-Is, suggesting sensitivity to fibroblast growth factor receptor inhibitors. It has been reported that alectinib, despite being a potent ALK-I, has limited inhibitory activity against other protein kinases such as FGFR2 (36). It may therefore be worth confirming whether the appearance of mutations in FGFR genes is a recurrent event after treatment failure with an ALK-I. If this proved to be the case, clinical trials evaluating the efficacy of combinations of ALK-Is with FGFR inhibitors would be of particular interest. Nevertheless, with respect to the FGFR2 mutation encountered, it is important to point out that although G305R has been identified in tumor samples (37, 38), it has not been biochemically characterized so, in this study, it was classified as being of unknown clinical significance.

Three CNVs in c-MYC, CCND1 and FGFR3 were detected upon disease progression in one patient, who was being treated with crizotinib. Remarkably, c-MYC amplification determines many oncogenic effects, including cell growth and proliferation (39) and it has been identified as a potential mechanism of primary resistance to crizotinib in ALK-rearranged NSCLC patients (40). It has been previously suggested by Alidousty et al that co-occurrence of early TP53 mutations in ALK + NSCLC can lead to chromosomal instability. Specifically, authors reported that, in a subset of 53 ALK + tumors, up to a quarter of TP53-mutated tumors showed amplifications of known cancer genes such as MYC or CCND1 (41). Consistent with this, we detected the P92A and V157F mutations in the TP53 gene in the same plasma sample of this patient.

Our results suggest that the P92A mutation in the TP53 gene could be of prognostic significance, although this observation should be interpreted with caution. Our data are consistent with those of previous studies. First of all, the median PFS was 11.6 months (95%CI: 6.5–20.9 months) for ALK-positive NSCLC patients treated with first-line crizotinib (N = 11) or alectinib (N = 2), which was very similar to that of the 10.9 months reported in the PROFILE 1014 trial, which included 172 patients randomized to crizotinib (42). When stratifying these patients according to the P92A mutation status, the median PFS was 7.7 months, for patients with tumors harboring the P92A mutation compared with 14.7 months for those in whom this mutation was not detected. Although this difference was not statistically significant. Similarly, Aisner et al recently reported that concomitant mutations in TP53 are associated with poorer survival among ALK + NSCLC patients (43). Likewise, TP53 mutations were identified as poor prognosis biomarkers in the phase 3 ALTA-1L trial (44).

Conclusions

In conclusion, we present a thorough molecular-level description of a series of patients with ALK-positive NSCLC progressing on an ALK-I. Molecular mechanisms underlying treatment failure seem to involve different pathways. NGS analysis of liquid biopsies collected upon disease progression is a valuable approach towards personalized that will lead to better care for ALK-positive NSCLC patients.

Abbreviations

AF

allele frequency
ALK
Anaplastic lymphoma kinase
ALK-Is
Anaplastic lymphoma kinase inhibitors
cfDNA
cell-free DNA
CNS
central nervous system
CNVs
copy-number variations
CSF
cerebrospinal fluid
dPCR
digital PCR
ECOG
Cooperative Oncology Group
IGV
Integrative Genomics Viewer
LOD
limit of detection
MAF
mutant allele frequency
MNP
multiple-nucleotide polymorphism
NGS
Next-generation sequencing
NPA
negative percentage agreement
NSCLC
non-small cell lung cancer
ORA
overall rates of agreement
OS
Overall survival
PFS
Progression-free survival
PPA
Positive percentage agreement
SNVs
single nucleotide variants
UMIs
unique molecular identifiers
WT
wild-type

Declarations

Ethics approval and consent to participate

The study protocol was approved by the Hospital Puerta de Hierro Ethics Committee (internal code 79-18), and was conducted in accordance with the precepts of the Code of Ethics of The World Medical Association (Declaration of Helsinki). All patients provided their appropriate written informed consent to participate in the study prior to enrollment.

Consent for publication

All named authors approved the content and submission to this journal.

Availability of data and materials

The datasets used and/or analysed during the current study are available from the corresponding author on reasonable request.

Competing interests:

MP reports personal fees from Roche, BMS, MSD Pfizer, Lilly, Novartis and Takeda grants and personal fees from AstraZeneca, and Boehringer during the conduct of the study. VC reports personal fees from Roche BMS, MSD, Pfizer, Lilly, AstraZeneca, Boehringer, Novartis, Takeda, during the conduct of the study. MD reports personal fees from Astra-Zeneca, BMS, Boehringer Ingelheim, MSD, Pfizer, Roche. The rest of the authors have declared no conflict of interest.

Funding:

This study has been funded by Instituto de Salud Carlos III through the project "PI17/01977" (Co-funded by European Regional Development Fund/European Social Fund "A way to make Europe"/"Investing in your future"). The work presented in this paper also received funding from the European Union's Horizon 2020 research and innovation programme under grant agreement No 875160.ES was funded by the Consejería de Ciencia, Universidades e Innovación of the Comunidad de Madrid (Doctorados Industriales of the Comunidad de Madrid IND2019/BMD-17258).RS was funded by the Consejería de Educación, Juventud y Deporte of the Comunidad de Madrid and by the Fondo Social Europeo (Programa Operativo de Empleo Juvenil, and Iniciativa de Empleo Juvenil, PEJD-2018-PRE/BMD-8640).

Author contributions

AR and MP conceived and /or designed the work. ES and RS have carried out statistical analyses. VI has developed VALK tool. All authors have made substantial contributions to the acquisition and interpretation of data. AR and ES have drafted and revised the manuscript. All authors have approved the final version. Each author agreed to be accountable for all aspects of the work in ensuring that questions related to the accuracy or integrity of any part of the work are appropriately investigated and resolved.

Acknowledgements

The authors wish to thank the donors, and the **BIOBANK HOSPITAL UNIVERSITARIO PUERTA DE HIERRO MAJADAHONDA (HUPHM) / INSTITUTO DE INVESTIGACIÓN SANITARIA PUERTA DE HIERRO-SEGOVIA DE ARANA (IDIPHISA) (PT17/0015/0020 in the Spanish National Biobanks Network)** for the human specimens used in this study".

References

1. Shaw AT, Yeap BY, Solomon BJ, Riely GJ, Gainor J, Engelman JA, et al. Effect of crizotinib on overall survival in patients with advanced non-small-cell lung cancer harbouring ALK gene rearrangement: A retrospective analysis. *Lancet Oncol.* 2011;12:1004–12.
2. Shaw AT, Kim DW, Nakagawa K, Seto T, Crinó L, Ahn MJ, et al. Crizotinib versus chemotherapy in advanced ALK-positive lung cancer. *N Engl J Med.* 2013;368:2385–94.
3. Gadgeel SM, Gandhi L, Riely GJ, Chiappori AA, West HL, Azada MC, et al. Safety and activity of alectinib against systemic disease and brain metastases in patients with crizotinib-resistant ALK-rearranged non-small-cell lung cancer (AF-002JG): Results from the dose-finding portion of a phase 1/2 study. *Lancet Oncol.* 2014;15:1119–28.
4. Duruisseaux M, Besse B, Cadranet J, Pérol M, Mennecier B, Bigay-Game L, et al. Overall survival with crizotinib and next-generation ALK inhibitors in ALK-positive non-small-cell lung cancer (IFCT-1302 CLINALK): A French nationwide cohort retrospective study. *Oncotarget.* 2017;8:21903–17.
5. Huber RM, Hansen KH, Paz-Ares Rodríguez L, West HL, Reckamp KL, Leighl NB, et al. Brigatinib in Crizotinib-Refractory ALK + NSCLC: 2-Year Follow-up on Systemic and Intracranial Outcomes in the Phase 2 ALTA Trial. *J Thorac Oncol.* 2020;15:404–15.
6. Peters S, Camidge DR, Shaw AT, Gadgeel S, Ahn JS, Kim DW, et al. Alectinib versus crizotinib in untreated ALK-positive non-small-cell lung cancer. *N Engl J Med.* 2017;377:829–38.
7. Camidge DR, Dziadziuszko R, Peters S, Mok T, Noe J, Nowicka M, et al. Updated Efficacy and Safety Data and Impact of the EML4-ALK Fusion Variant on the Efficacy of Alectinib in Untreated ALK-Positive Advanced Non-Small Cell Lung Cancer in the Global Phase III ALEX Study. *J Thorac Oncol.* 2019;14:1233–43.
8. Lin JJ, Zhu VW, Yoda S, Yeap BY, Schrock AB, Dagogo-Jack I, et al. Impact of EML4-ALK variant on resistance mechanisms and clinical outcomes in ALK-positive lung cancer. *J Clin Oncol.* 2018;36:1199–206.
9. Doebele RC, Pilling AB, Aisner DL, Kutateladze TG, Le AT, Weickhardt AJ, et al. Mechanisms of resistance to crizotinib in patients with ALK gene rearranged non-small cell lung cancer. *Clin Cancer Res.* 2012;18:1472–82.
10. Katayama R, Shaw AT, Khan TM, Mino-Kenudson M, Solomon BJ, Halmos B, et al. Cancer: Mechanisms of acquired crizotinib resistance in ALK-rearranged lung cancers. *Sci Transl Med.* 2012;4:120ra17.
11. Gainor JF, Dardaei L, Yoda S, Friboulet L, Leshchiner I, Katayama R, et al. Molecular mechanisms of resistance to first- and second-generation ALK inhibitors in ALK-rearranged lung cancer. *Cancer Discov* 2016.
12. Okada K, Araki M, Sakashita T, Ma B, Kanada R, Yanagitani N, et al. Prediction of ALK mutations mediating ALK-TKIs resistance and drug re-purposing to overcome the resistance. *EBioMedicine.* 2019;41:105–19.
13. Li J, Huang Y, Wu M, Wu C, Li X, Bao J. Structure and energy based quantitative missense variant effect analysis provides insights into drug resistance mechanisms of anaplastic lymphoma kinase mutations. *Sci Rep.* 2018;8:10664.
14. Ettinger DS, Wood DE, Aisner DL, Akerley W, Bauman J, Chirieac LR, et al. Non-small cell lung cancer, version 5.2017: Clinical practice guidelines in oncology. *J Natl Compr Canc Netw.* 2017;15:504–35.

15. Provencio M, Pérez-Barrios C, Barquin M, Calvo V, Franco F, Sánchez E, et al. Next-generation sequencing for tumor mutation quantification using liquid biopsies. *Clin Chem Lab Med*. 2020;58:306–13.
16. Li MM, Datto M, Duncavage EJ, Kulkarni S, Lindeman NI, Roy S, et al. Standards and Guidelines for the Interpretation and Reporting of Sequence Variants in Cancer. *J Mol Diagn*. 2017;19:4–23.
17. Gambacorti Passerini C, Farina F, Stasia A, Redaelli S, Ceccon M, Mologni L, et al. Crizotinib in advanced, chemoresistant anaplastic lymphoma kinase-positive lymphoma patients. *J Natl Cancer Inst*. 2014;106:djt378.
18. Hug H, Schuler R. Measurement of the number of molecules of a single mRNA species in a complex mRNA preparation. *J Theor Biol*. 2003;221:615–24.
19. Kivioja T, Vähärautio A, Karlsson K, Bonke M, Enge M, Linnarsson S, et al. Counting absolute numbers of molecules using unique molecular identifiers. *Nat Methods*. 2011;9:72–4.
20. Yanagitani N, Uchibori K, Koike S, Tsukahara M, Kitazono S, Yoshizawa T, et al. Drug resistance mechanisms in Japanese anaplastic lymphoma kinase-positive non-small cell lung cancer and the clinical responses based on the resistant mechanisms. *Cancer Sci*. 2020;111:932–9.
21. Horn L, Whisenant JG, Wakelee H, Reckamp KL, Qiao H, Leal TA, et al. Monitoring Therapeutic Response and Resistance: Analysis of Circulating Tumor DNA in Patients With ALK + Lung Cancer. *J Thorac Oncol*. 2019;14:1901–11.
22. Noé J, Lovejoy A, Ou SHI, Yaung SJ, Bordogna W, Klass DM, et al. ALK Mutation Status Before and After Alectinib Treatment in Locally Advanced or Metastatic ALK-Positive NSCLC: Pooled Analysis of Two Prospective Trials. *J Thorac Oncol*. 2020;15:601–8.
23. Dagogo-Jack I, Rooney M, Lin JJ, Nagy RJ, Yeap BY, Hubbeling H, et al. Treatment with Next-Generation ALK Inhibitors Fuels Plasma ALK Mutation Diversity. *Clin Cancer Res*. 2019;25:6662–70.
24. Romero A, Serna-Blasco R, Alfaro C, Sánchez-Herrero E, Barquín M, Turpin MC, et al. ctDNA analysis reveals different molecular patterns upon disease progression in patients treated with osimertinib. *Transl Lung Cancer Res*. 2020;9:532–40.
25. Wang F, Travins J, DeLaBarre B, Penard-Lacronique V, Schalm S, Hansen E, et al. Targeted inhibition of mutant IDH2 in leukemia cells induces cellular differentiation. *Science*. 2013;340:622–6.
26. Mylonas E, Janin M, Bawa O, Opolon P, David M, Quivoron C, et al. Isocitrate dehydrogenase (IDH)2 R140Q mutation induces myeloid and lymphoid neoplasms in mice. *Leukemia*. 2014;28:1343–6.
27. Cairns RA, Iqbal J, Lemonnier F, Kucuk C, De Leval L, Jais JP, et al. IDH2 mutations are frequent in angioimmunoblastic T-cell lymphoma. *Blood*. 2012;119:1901–3.
28. Rodriguez EF, De Marchi F, Lokhandwala PM, Belchis D, Xian R, Gocke CD, et al. IDH1 and IDH2 mutations in lung adenocarcinomas: Evidences of subclonal evolution. *Cancer Med*. 2020;9:4386–94.
29. Boland JM, Jang JS, Li J, Lee AM, Wampfler JA, Erickson-Johnson MR, et al. MET and EGFR mutations identified in ALK-rearranged pulmonary adenocarcinoma: Molecular analysis of 25 ALK-positive cases. *J Thorac Oncol*. 2013;8:574–81.
30. Tiseo M, Gelsomino F, Boggiani D, Bortesi B, Bartolotti M, Bozzetti C, et al. EGFR and EML4-ALK gene mutations in NSCLC: A case report of erlotinib-resistant patient with both concomitant mutations. *Lung Cancer*. 2011;71:241–3.
31. Verdusco D, Kuenzi BM, Kinose F, Sondak VK, Eroglu Z, Rix U, et al. Ceritinib enhances the efficacy of trametinib in BRAF/NRAS-wild-type melanoma cell lines. *Mol Cancer Ther*. 2018;17:73–83.
32. Wang H, Daouti S, Li WH, Wen Y, Rizzo C, Higgins B, et al. Identification of the MEK1(F129L) activating mutation as a potential mechanism of acquired resistance to MEK inhibition in human cancers carrying the B-Raf V600E mutation. *Cancer Res*. 2011;71:5535–45.
33. Hrustanovic G, Bivona TG. RAS-MAPK in ALK targeted therapy resistance. *Cell Cycle*. 2015;14:3661–2.
34. Hrustanovic G, Olivás V, Pazarentzos E, Tulpule A, Asthana S, Blakely CM, et al. RAS-MAPK dependence underlies a rational polytherapy strategy in EML4-ALK-positive lung cancer. *Nat Med*. 2015;21:1038–47.
35. Crystal AS, Shaw AT, Sequist LV, Friboulet L, Niederst MJ, Lockerman EL, et al. Patient-derived models of acquired resistance can identify effective drug combinations for cancer. *Science*. 2014;346:1480–6.
36. Sakamoto H, Tsukaguchi T, Hiroshima S, Kodama T, Kobayashi T, Fukami TA, et al. CH5424802, a Selective ALK Inhibitor Capable of Blocking the Resistant Gatekeeper Mutant. *Cancer Cell*. 2011;19:679–90.
37. Gartside MG, Chen H, Ibrahim OA, Byron SA, Curtis AV, Wellens CL, et al. Loss-of-function fibroblast growth factor receptor-2 mutations in melanoma. *Mol Cancer Res*. 2009;7:41–54.
38. Haugh AM, Zhang B, Quan VL, Garfield EM, Bublej JA, Kudalkar E, et al. Distinct Patterns of Acral Melanoma Based on Site and Relative Sun Exposure. *J Invest Dermatol*. 2018;138:384–93.
39. Lin CY, Lovén J, Rahl PB, Paranal RM, Burge CB, Bradner JE, et al. Transcriptional amplification in tumor cells with elevated c-Myc. *Cell*. 2012;151:56–67.
40. Rihawi K, Alfieri R, Fiorentino M, Fontana F, Capizzi E, Cavazzoni A, et al. MYC Amplification as a Potential Mechanism of Primary Resistance to Crizotinib in ALK-Rearranged Non-Small Cell Lung Cancer: A Brief Report. *Transl Oncol*. 2019;12:116–21.
41. Alidousty C, Baar T, Martelotto LG, Heydt C, Wagener S, Fassunke J, et al. Genetic instability and recurrent MYC amplification in ALK-translocated NSCLC: a central role of TP53 mutations. *J Pathol*. 2018;246:67–76.
42. Solomon BJ, Mok T, Kim D-W, Wu Y-L, Nakagawa K, Mekhail T, et al. First-Line Crizotinib versus Chemotherapy in ALK-Positive Lung Cancer. *N Engl J Med*. 2014;371:2167–77.
43. Aisner DL, Sholl LM, Berry LD, Rossi MR, Chen H, Fujimoto J, et al. The impact of smoking and tp53 mutations in lung adenocarcinoma patients with targetable mutations—the lung cancer mutation consortium (LCMC2). *Clin Cancer Res*. 2018;24:1038–47.

Figures

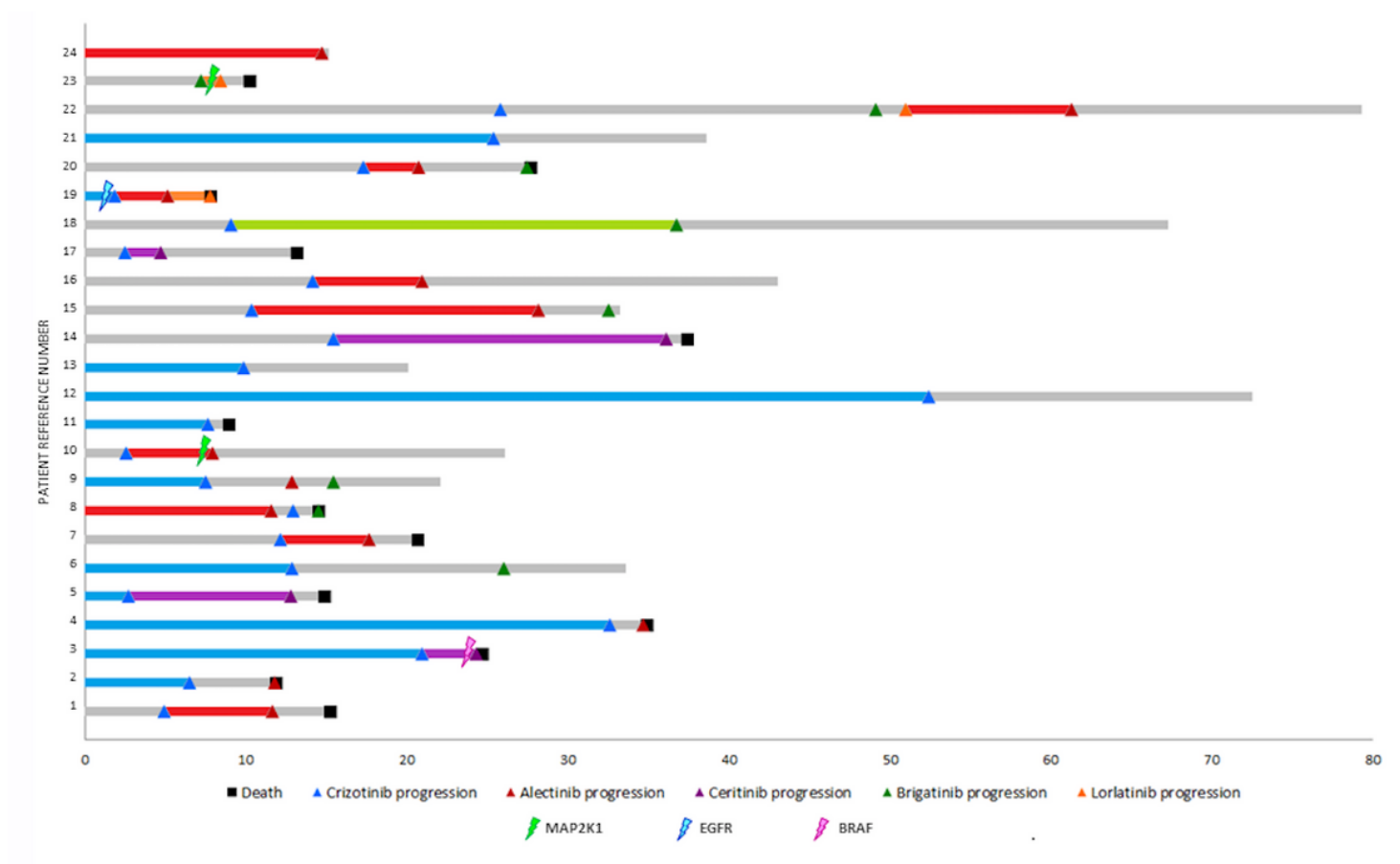


Figure 1
Swimmer chart showing the individual treatment responses of the study cohort. Blue, red, purple, green and orange bars correspond to patients who were treated with crizotinib, alectinib, ceritinib, brigatinib and lorlatinib, respectively. Tumor progression is denoted by triangle and patient's death is denoted by a square. Mutations in BRAF, EGFR and MAP2K are indicated by a lightning.

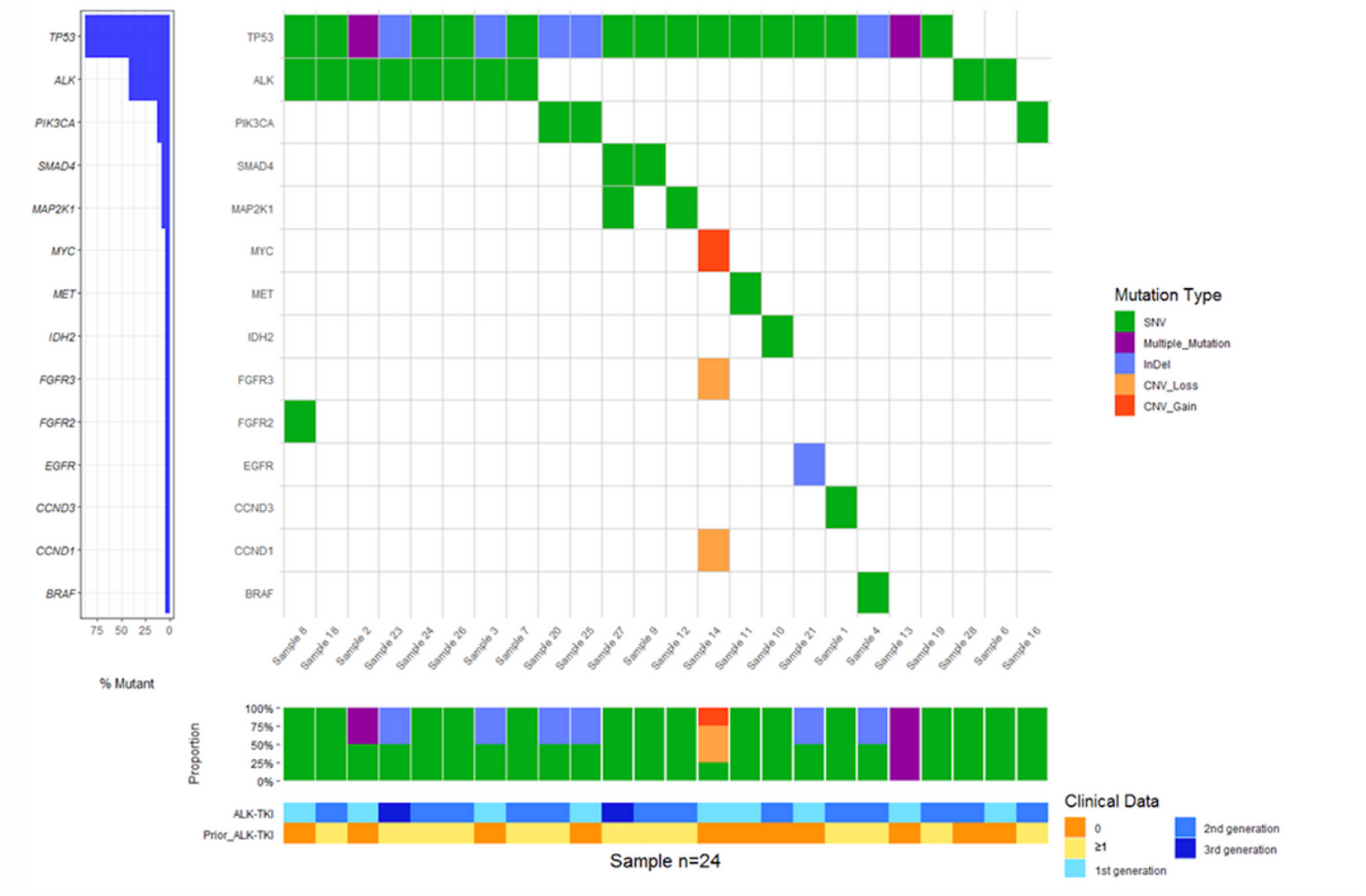


Figure 2

Co-mutation plot according to ctDNA profiling by NGS. Each column represents data from a single patient. Each row represent data from a specific gene. Indels are represented in blue whereas missense mutations are represented in green. CNVs are colored in orange. Heatmap at the bottom illustrates type of treatment received.

Supplementary Files

This is a list of supplementary files associated with this preprint. Click to download.

- [S3.xlsx](#)
- [S2.xlsx](#)
- [S1.xlsx](#)
- [S4.pptx](#)
- [S3.pptx](#)
- [S2.pptx](#)
- [S1.pptx](#)
- [SuppMat.pdf](#)